The Parkinson's Disease-Associated H50Q Mutation Accelerates α-Synuclein Aggregation in Vitro

ARTICLE *in* BIOCHEMISTRY · SEPTEMBER 2013

Impact Factor: 3.02 · DOI: 10.1021/bi400999d · Source: PubMed

10 AUTHORS, INCLUDING:

Dhiman Ghosh
Indian Institute of Technology Bombay
13 PUBLICATIONS **96** CITATIONS
SEE PROFILE

Pradeep Kumar Singh
The Rockefeller University
23 PUBLICATIONS **188** CITATIONS
SEE PROFILE

Anoop Arunagiri
University of Michigan
12 PUBLICATIONS **128** CITATIONS
SEE PROFILE

Samir Maji
Indian Institute of Technology Bombay
69 PUBLICATIONS **1,842** CITATIONS
SEE PROFILE

BIOCHEMISTRY
including biophysical chemistry & molecular biology

Rapid Report

pubs.acs.org/biochemistry

The Parkinson's Disease-Associated H50Q Mutation Accelerates α-Synuclein Aggregation *in Vitro*

Dhiman Ghosh, Mrityunjoy Mondal, Ganesh M. Mohite, Pradeep K. Singh, Priyatosh Ranjan, A. Anoop, Saikat Ghosh, Narendra Nath Jha, Ashutosh Kumar, and Samir K. Maji*

Department of Biosciences and Bioengineering, IIT Bombay, Powai, Mumbai, India 400076

Supporting Information

ABSTRACT: α-Synuclein (α-Syn) aggregation is directly linked with Parkinson's disease (PD) pathogenesis. Here, we analyzed the aggregation of newly discovered α-Syn missense mutant H50Q *in vitro* and found that this mutation significantly accelerates the aggregation and amyloid formation of α-Syn. This mutation, however, did not alter the overall secondary structure as suggested by two-dimensional nuclear magnetic resonance and circular dichroism spectroscopy. The initial oligomerization study by cross-linking and chromatographic techniques suggested that this mutant oligomerizes to an extent similar to that of the wild-type α-Syn protein. Understanding the aggregation mechanism of this H50Q mutant may help to establish the aggregation and phenotypic relationship of this novel mutant in PD.

The major neuropathological hallmark of Parkinson's disease (PD) is the presence of insoluble fibrous aggregates, composed of 140-residue protein α-synuclein (α-Syn), in intraneuronal inclusions of Lewy bodies (LBs) and Lewy neurites (LNs).[1] The discovery of three familial PD disease-related mutants of α-Syn (A30P, A53T, and E46K) and their effects on the *in vitro* aggregation profile support the role of α-Syn aggregation in PD pathogenesis.[2,3] Although A53T and E46K mutations accelerate α-Syn aggregation *in vitro*, the A30P mutation decreases the overall rate of fibril formation.[3,4] Recent studies have suggested that soluble, oligomeric, fibril precursors of α-Syn are potent neurotoxins that may be the most potent pathogenic entity of PD.[5,6] Therefore, understanding the α-Syn assembly dynamics and structure of the assemblies could be important for the development of effective therapeutic agents against the disease.[3] Recently, two new familial α-Syn mutations have been discovered, H50Q[7,8] and G51D,[9,10] which are associated with early onset pathogenesis of PD and multiple-system atrophy (MSA) (for G51D). The aggregation study of the G51D mutant suggested its slower rate of oligomerization compared to that of the wild type.[10] However, aggregation and amyloid formation of H50Q *in vitro* have not yet been documented. In this report, we investigate the aggregation of the H50Q mutation along with wild-type (wt) α-Syn using various biophysical techniques, including circular dichroism (CD) for structural conversion and thioflavin T (ThT) fluorescence for determining aggregation kinetics. Electron microscopy (EM) and atomic force microscopy (AFM) were used for morphological characterization of protein aggregates.

The effect of a single point mutation (H50Q) on the secondary structure of α-Syn was studied using two-dimensional nuclear magnetic resonance (NMR) spectroscopy. Two mutants (H50Q and H50A) were created by site-directed mutagenesis (Supporting Information). Proteins were expressed and purified using a protocol established previously (Supporting Information). We prepared the low-molecular weight (LMW) forms of all proteins at 300 μM in aggregation buffer [20 mM Gly-NaOH (pH 7.4) and 0.01% sodium azide] and incubated them at 37 °C with slight agitation. At regular intervals, CD and ThT binding were performed. The kinetics determined by the ThT binding data suggests that proteins aggregated through nucleation-dependent polymerization (Figure 1A). The lag time for wt was 60 ± 4 h and for H50Q was 40 ± 5 h, indicating H50Q substantially accelerated the aggregation kinetics (Figure 1A, inset). We also investigated the H50A mutant to delineate whether His50 and/or its mutation to glutamine (Q) is an important factor for accelerating the aggregation. The aggregation kinetics of H50A was also faster (lag

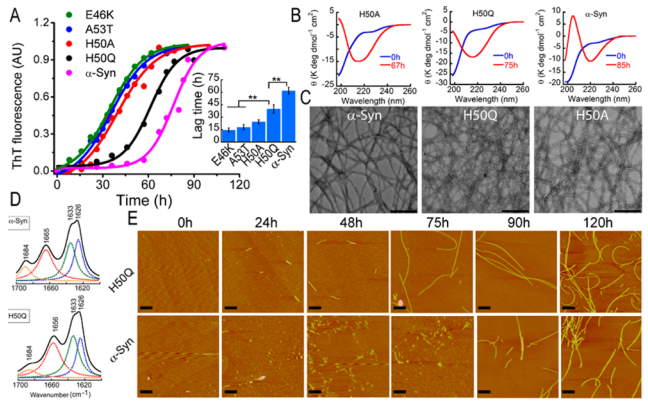

Figure 1. Fibrillation of α-Syn, H50Q, and H50A. (A) Kinetics of α-Syn and its mutants measured by ThT fluorescence. Lag times of corresponding fibril formation are shown in the inset. (B) CD spectroscopy showing the conformational transition of random coil to β-sheet during fibrillation. (C) EM images of aged fibrils of wt α-Syn and its mutants. (D) Fourier transform infrared spectroscopy of α-Syn and H50Q fibrils showing the predominant β-sheet conformation in fibrils. (E) Time-dependent AFM kinetics of α-Syn and H50Q showing the development of fibrils. H50Q showed a faster appearance of filaments than wt. Scale bars are 500 nm.

Received: July 27, 2013
Revised: September 18, 2013
Published: September 18, 2013

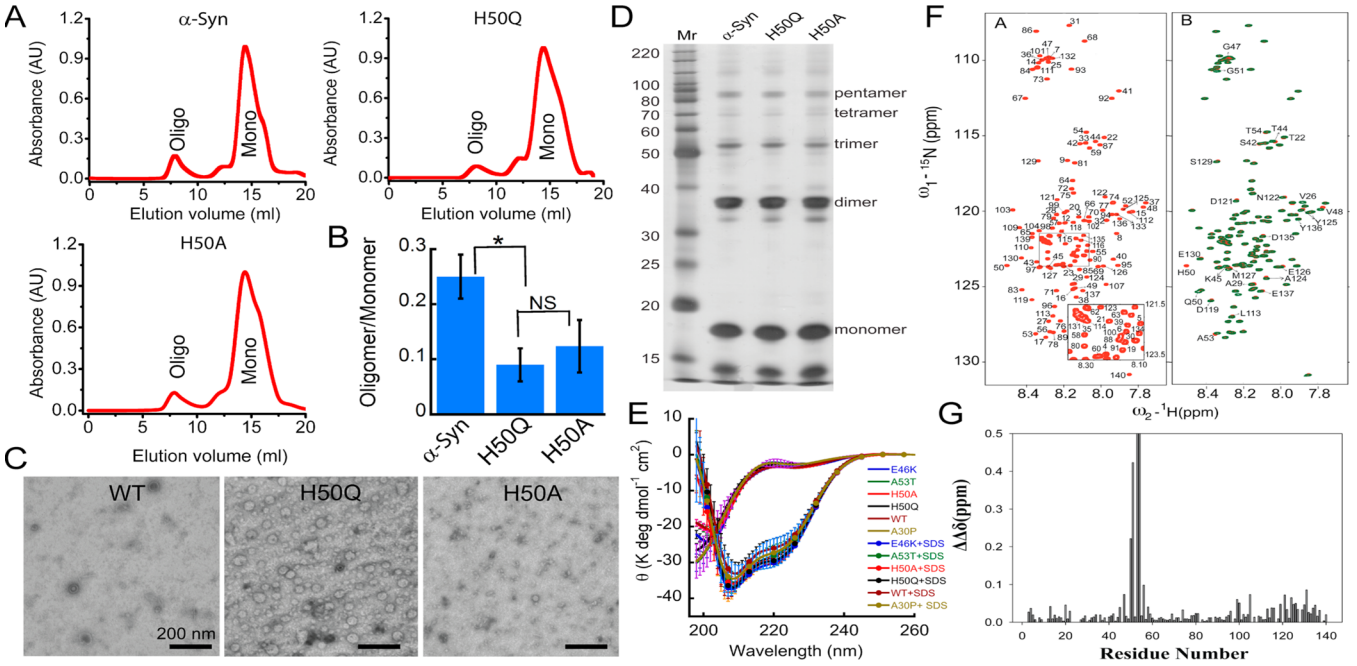

Figure 2. Biophysical characterization of monomeric and oligomeric species of α-Syn and its H50Q and H50A mutants. (A) Size exclusion profile of α-Syn and its H50Q and H50A mutants showing their corresponding oligomeric and monomeric elution peak. (B) Bar diagram representation of the area of the oligomer/monomer ratio showing a larger amount of oligomer appeared for α-Syn than for H50Q. (C) EM images of oligomers of synucleins isolated via size exclusion chromatography. (D) Sodium dodecyl sulfate−polyacrylamide gel electrophoresis image of cross-linked (PICUP) products of synucleins. (E) CD spectroscopy of LMW synucleins (100 kDa) in the presence and absence of 0.5% (v/v) SDS showing no significant secondary structural differences between wt and H50Q. (F) Well-resolved heteronuclear single-quantum coherence (HSQC) spectra of LMW wt α-Syn (left). Peaks were assigned using published $^{1}H-^{15}N$ chemical shift values (BMRB accession number 16543) and were further confirmed with the help of three-dimensional total correlation spectroscopy-HSQC. Overlaid $^{1}H-^{15}N$ HSQC spectra of wt α-Syn and the H50Q mutant (right). (G) Chemical shift perturbations between wt α-Syn and H50Q. Significant chemical shift perturbations were seen for the residues near the mutation site around residues 44−56 and the C-terminal residues (113−135).

time of 22 ± 3 h), indicating replacement of His50 mostly affects the kinetics. To compare the acceleration of aggregation, we also studied two other faster-aggregating PD familial disease-associated mutants. The data indicate that H50Q and H50A aggregate more quickly than wt but more slowly than A53T and E46K. Further, CD spectroscopy revealed that after immediate preparation of LMW forms, all synucleins were unstructured (Figure 1B and Figure S1A of the Supporting Information). However, upon incubation, they converted to β-sheet depending upon their aggregation kinetics.

Morphological analysis using EM suggests that all α-Syn-formed amyloid fibrils, where mostly two protofilaments contributing to H50Q fibrils, whereas, wt, E46K, H50A, and A53T fibrils consisted of more than two filaments (Figure 1C and Figure S1B of the Supporting Information). The secondary structure of wt and H50Q fibrils determined by Fourier transform infrared spectroscopy showed the most intense peak at 1626 cm^{-1} along with a weak peak at 1684 cm^{-1} suggesting antiparallel β-sheet formation (Figure 1D). The oligomerization and fibril development of H50Q and wt protein were further studied using AFM during the course of aggregation. Both proteins showed oligomerization through small oligomers, from protofibrils to fibrils (Figure 1E). No unusual accumulation of oligomers was seen for H50Q. However, H50Q formed higher-order filaments faster than wt. Therefore, the data suggest that H50Q accelerates the aggregation of α-Syn fibrillation. Further, we tested the cellular toxicity of 30 μM fibril form of wt, A30P, E46K, H50A, H50Q, and A53T using the MTT assay. Although α-Syn is known to aggregate intracellularly, an extracellular toxicity model such as the MTT assay is routinely used for toxicity measurements.[10] Here, we used the SH-SY5Y cell line as an extracellular model for the MTT assay. The data suggest that wt and mutant fibrils are toxic to SH-SY5Y cells upon being added extracellularly (Figure S2A of the Supporting Information). However, in the MTT assay, all the fibrils exhibited similar toxicity. We also assessed the generation of intracellular reactive oxygen species (ROS) in SH-SY5Y cells after they had been treated with wt and mutant fibrils. All these fibrils also generate similar levels of ROS (Figure S2B and results of the Supporting Information).

In light of recent suggestions that early formed α-Syn oligomers might be most possible toxic species in PD,[5,6] we analyzed whether the H50Q mutation accelerates early oligomerization of α-Syn. Two different techniques [size exclusion chromatography (SEC)[5] and photoinduced cross-linking of unmodified protein (PICUP)[11]] were used to probe the early oligomerization of both proteins. For the SEC study, 10 mg/mL wt α-Syn, H50Q, and H50A were solubilized in PBS (pH 7.4) and centrifuged at 14000g for 30 min. After centrifugation, 500 μL of the supernatant was injected onto the SEC column. Figure 2A shows the normalized SEC chromatograms of all three proteins with monomeric and oligomeric fractions. The monomer and oligomer elution peak volumes were integrated to calculate the oligomer/monomer ratio. We found the oligomer/monomer ratio is lower for H50Q and H50A than for wt α-Syn (Figure 2B), suggesting relatively less formation of preformed oligomers for H50Q and H50A. EM images of α-Syn oligomers isolated from SEC revealed various types of oligomers were omnipresent, including spherical oligomers, wormlike protofibrils, and porelike structure. How-

dx.doi.org/10.1021/bi400999d | Biochemistry 2013, 52, 6925−6927

ever, for an unknown reason, H50Q exhibited a denser population of spherical and porelike structures under EM (Figure 2C).

The early oligomerization propensities of these proteins were further probed using PICUP.[11] The 100 kDa LMW proteins were cross-linked, and products were analyzed using sodium dodecyl sulfate−polyacrylamide gel electrophoresis to visualize resulting oligomer distributions. The data showed monomeric to pentameric species without any significant population differences of each species across three different proteins (Figure 2D). EM analysis of both cross-liked (+PICUP) and un-cross-linked (−PICUP) samples showed mostly amorphous or small globular structures. However, after cross-linking, all proteins formed relatively larger clumps than non-cross-linked samples (Figure S3 of the Supporting Information).

To address the possible effect on secondary structure due to the H50Q mutation and its probable implication in aggregation kinetics, secondary structure analysis of all three synucleins was performed in buffer with and without 0.5% SDS using CD spectroscopy. In this study, we also included three other familial disease mutants (A30P, E46K, and A53T). SDS was used to mimic the membrane environment for structural analysis. The CD data showed random coil and helix conformations of all three proteins in buffer and SDS, respectively, without any significant differences (Figure 2E). The data suggest that neither H50Q nor H50A altered the major secondary structure under normal physiological conditions or membrane mimicking conditions. To further study the effect of mutation in residue specific detail, a two-dimensional NMR study [heteronuclear single-quantum coherence (HSQC)] was performed with 30 kDa LMW wt and H50Q in 20 mM sodium phosphate buffer (pH 6.0). Consistent with CD data, NMR data also revealed mostly unstructured conformations of both wt and H50Q without significant structural changes caused by the H50Q mutation. However, the residue specific assignment of both spectra and their overlay suggest chemical shift perturbations of H50Q for the residues near the site of mutation around residues 44−56 and the C-terminal residues (113−135) (Figure 2F,G) compared to those of wt. The data suggest that the H50Q mutation may modulate the interactions between the NAC region and the C-terminus as reported previously.[12] Moreover, previous computational studies have shown that all three PD-associated mutants alter long-range interactions mediated by NAC and the N- and C-termini of α-Syn in the monomeric state.[13−15]

In conclusion, our data suggest that the PD disease-associated H50Q mutation[7,8] significantly accelerates α-Syn aggregation without altering the major secondary structure or early oligomer-forming tendency. This alteration is not due to the mutation of His to Gln but rather the replacement of His50. The chemical shift perturbations observed at the H50Q mutation site and at the C-terminus suggest that subtle structural changes caused by mutation might account for the altered aggregation kinetics. The mechanistic study of aggregation of wt and H50Q may improve our understanding of the aggregation phenotypic relationship of the H50Q mutant in PD pathogenesis. Furthermore, His50 of α-Syn is one of the important residues for Cu(II) binding,[16] and therefore, its replacement in the H50Q mutant may affect the secondary structure in the presence of Cu(II),[8] which may potentially modulate pathology in PD.

■ ASSOCIATED CONTENT

Supporting Information

Detailed description of material methods and supplementary figures. This material is available free of charge via the Internet at http://pubs.acs.org.

■ AUTHOR INFORMATION

Corresponding Author

*Department of Biosciences and Bioengineering, IIT Bombay, Powai, Mumbai, India 400076. Phone: 91-22-2576-7774. E-mail: samirmaji@iitb.ac.in. Fax: 91-22-2572 3480.

Author Contributions

S.K.M. designed the experiments. All authors except S.K.M. performed the experiments. All authors analyzed data. S.K.M. wrote the manuscript.

Author Contributions

D.G. and M.M. contributed equally to this work.

Funding

The work was supported by grants from DBT (BT/PR14344Med/30/501/2010 and BT/PR13359/BRB/10/752/2009), DST (SR/FR/LS-032/2009), CSIR [37(1404)/10/EMR-11], and ICMR [5/20/9 (Bio)/II-NCD-I], Government of India. A.K. is thankful for a Ramalingaswami fellowship.

Notes

The authors declare no competing financial interests.

■ ACKNOWLEDGMENTS

We acknowledge the Central SPM and EM Facility (IRCC, IIT Bombay). We thank the National Facility for High-Field NMR at TIFR.

■ REFERENCES

(1) Goedert, M. (2001) *Nat. Rev. Neurosci. 2*, 492−501.
(2) Cookson, M. R. (2005) *Annu. Rev. Biochem. 74*, 29−52.
(3) Lashuel, H. A., Overk, C. R., Oueslati, A., and Masliah, E. (2013) *Nat. Rev. Neurosci. 14*, 38−48.
(4) Conway, K. A., Lee, S. J., Rochet, J. C., Ding, T. T., Williamson, R. E., and Lansbury, P. T. (2000) *Proc. Natl. Acad. Sci. U.S.A. 97*, 571−576.
(5) Winner, B., et al. (2011) *Proc. Natl. Acad. Sci. U.S.A. 108*, 4194−4199.
(6) Karpinar, D. P., et al. (2009) *EMBO J. 28*, 3256−3268.
(7) Appel-Cresswell, S., et al. (2013) *Mov. Disord. 28*, 811−813.
(8) Proukakis, C., Dudzik, C. G., Brier, T., MacKay, D. S., Cooper, J. M., Millhauser, G. L., Houlden, H., and Schapira, A. H. (2013) *Neurology 80*, 1062−1064.
(9) Kiely, A. P., Asi, Y. T., Kara, E., Limousin, P., Ling, H., Lewis, P., Proukakis, C., Quinn, N., Lees, A. J., Hardy, J., Revesz, T., Houlden, H., and Holton, J. L. (2013) *Acta Neuropathol. 125*, 753−769.
(10) Lesage, S., Anheim, M., Letournel, F., Bousset, L., Honore, A., Rozas, N., Pieri, L., Madiona, K., Durr, A., Melki, R., Verny, C., and Brice, A. (2013) *Ann. Neurol. 73*, 459−471.
(11) Bitan, G., and Teplow, D. B. (2004) *Acc. Chem. Res. 37*, 357−364.
(12) Bertoncini, C. W., Jung, Y. S., Fernandez, C. O., Hoyer, W., Griesinger, C., Jovin, T. M., and Zweckstetter, M. (2005) *Proc. Natl. Acad. Sci. U.S.A. 102*, 1430−1435.
(13) Coskuner, O., and Wise-Scira, O. (2013) *ACS Chem. Neurosci. 4*, 1101−1113.
(14) Wise-Scira, O., Aloglu, A. K., Dunn, A., Sakallioglu, I. T., and Coskuner, O. (2013) *ACS Chem. Neurosci. 4*, 486−497.
(15) Wise-Scira, O., Dunn, A., Aloglu, A. K., Sakallioglu, I. T., and Coskuner, O. (2013) *ACS Chem. Neurosci. 4*, 498−508.
(16) Dudzik, C. G., Walter, E. D., and Millhauser, G. L. (2011) *Biochemistry 50*, 1771−1777.